

Drop Impact Simulation on Heated Structured Surfaces

N. Samkhaniani, M. Toprak, A. Stroh

¹Institute of Fluid Mechanics/Karlsruhe Institute of Technology (KIT)
Kaiserstr. 10, 76131 Karlsruhe, Germany
nima.samkhaniani@kit.edu

Abstract - In this study, hydrodynamics and heat transfer of a droplet (in mm range) impinging on a heated superhydrophobic surface with subsequent bouncing are investigated. The simulations are conducted with in-house solver *phaseFieldFoam*, extended to implicitly account for air entrapment on superhydrophobic micro-texture. The result shows the Dirichlet boundary condition can be also employed for Cassie-Baxter condition without any major error and air entrapment has negligible effect on heat transfer from the surface.

Keywords: hydrophobic surfaces, heat transfer, drop impact, phase field method, OpenFOAM

1. Introduction

Heat transfer on drop impact is important for various industrial applications such as spray cooling and fuel injection [1] or injection of urea-water solution sprays into automotive exhaust pipes for selective catalytic reduction [2]. Various parameters such as drop diameter (d_0), drop impact velocity (V_0), gas-liquid surface tension (σ) determine the droplet behaviour after impact on the smooth surface. The main characteristic non-dimensional number for the process is the Weber number $We = \rho V_0^2 d_0 / \sigma$. Another influential parameter is the surface wettability, which represents the surface ability to be wetted and is mainly determined by the surface roughness and its topography. The effect of surface wettability can be considered via static contact angle θ_e . Surfaces in contact with the water droplet can be classified into hydrophilic ($\theta_e < 90$) and hydrophobic ($\theta_e > 90$) surfaces. Surface structure directly affects the surface wettability whereas surfaces fabricated with micro/nano textures can also become super-hydrophobic ($\theta_e > 130$).

In the case of a hot, dry solid surface, the droplet impact outcomes are classified into several regimes: evaporation, nucleate boiling, foaming, transitional boiling, and film boiling [3]. Roisman [4] pointed out that evaporation is negligible during the spreading and receding stages of bouncing droplets in the film evaporation regime. The outcome of drop impingement in low weber number in the film evaporation regime is thoroughly investigated in our previous study [5]. We showed that in the rebounding regime increasing the weber number increases the cooling effectiveness on a smooth surface. The objective of the present study is to understand how structured patterns affect heat transfer during such process. The surface structuring increases the effective area during the droplet impingement resulting in an increase in the heat transfer, while air entrapment in cavities may impair the heat transfer rate compared to a drop impact on a smooth surface. In order to understand the effect of surface structure on heat transfer, a new boundary condition is implemented to implicitly consider the effect of the air entrapment. To the authors' best knowledge, the heat transfer during the impact of a single droplet on a superhydrophobic surface has not been investigated before. In the present study, this phenomenon is simulated with the in-house solver *phaseFieldFoam*.

2. Governing Equations

The present computations are performed by a phase field method with the coupled Cahn-Hilliard-Navier-Stokes equations for two incompressible and immiscible phases being solved by OpenFOAM-extend. For details on governing equations, numerical implementation and validation of the solver *phaseFieldFoam* the reader is referred to [5,6]. Two boundary conditions for temperature at solid surface are considered:

$$T_f = T_s, \quad (1)$$

$$T_f = \frac{2k_c T_c H_p + k_{eff} T_s \Delta x}{2k_c H_p + k_{eff} \Delta x}. \quad (2)$$

Where Eq.1 is a Dirichlet boundary condition applying a fixed temperature (T_s) at the bottom structured surface. In Eq.2 the surface temperature (T_f) is obtained via an energy flux balance around the solid-liquid interface. The pore cavity is here considered in the surface thermal conductivity (k_{eff}) as shown in Fig.1.

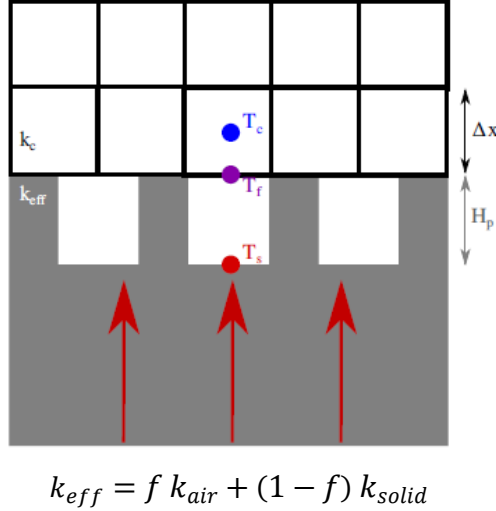


Fig.1: Description of implicit boundary condition which accounts the pore cavity, f is pore fraction.

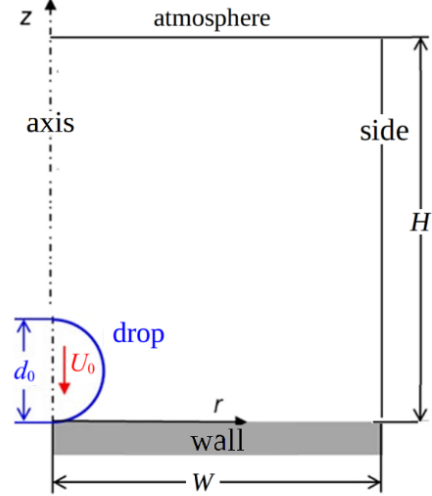


Fig.2: Schematic representation of computational setup for drop impact on solid surface $[W \times H] = 1.5d_0 \times 7.5d_0$

3. Result and discussion

3.1. Problem definition

The schematic of the problem is shown in Fig.2. At the bottom wall, no slip condition and fixed contact angle $\theta_e = 140$ are applied, while temperature boundary condition corresponds to Eq.1 or 2. At the atmosphere boundary, the *totalPressure* with homogeneous Neumann boundary conditions for velocity and order parameter are used. The grid is created with the OpenFOAM mesh generator *blockMesh*. The domain utilizes 150×750 uniform cells with size corresponding to Cahn number $Cn = \xi/d_0$ where 4ξ is the interface thickness resolves with 8 cells. The physical properties of drop, air and solid are given in Table 1. In the interface region, the physical properties $\varphi \in [\mu, \rho, c_p, k]$ are calculated through arithmetic interpolation $\varphi = \left(\frac{1+c}{2}\right)\varphi_l + \left(\frac{1-c}{2}\right)\varphi_g$, where order parameter $c = [-1, 1]$.

Table 1: Thermophysical properties [7]

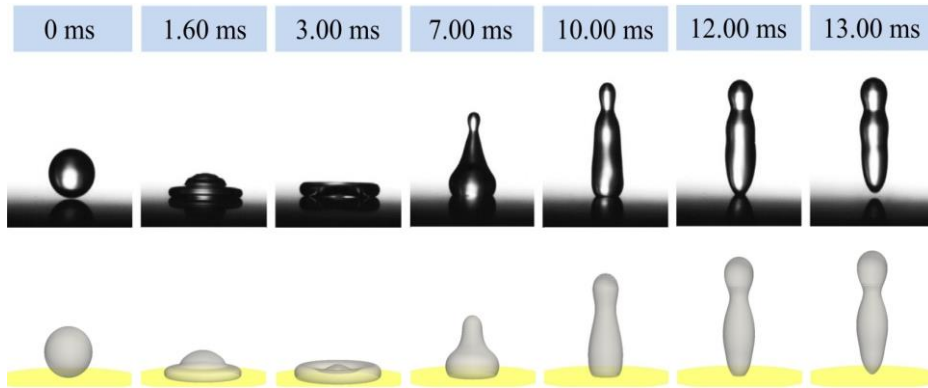
	μ [Pa.s]	ρ [kg/m ³]	c_p [J/kg K]	k [W/m K]	σ [N/m]
Liquid (water)	9.01×10^{-4}	998	4200	0.6	0.072
Gas (air)	1.48×10^{-5}	1.29	1006	0.026	
Solid		2329	700	120	

3.2 Validation

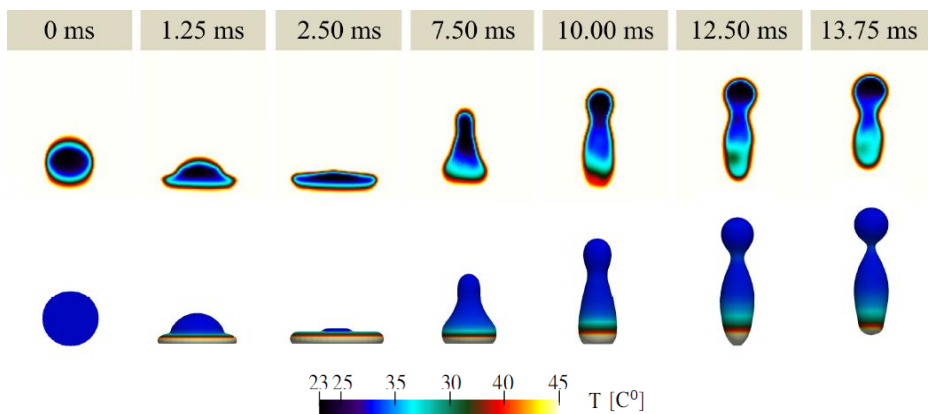
In Fig. 3-a, the sequence of drop impact ($d_0 = 2.3$ mm, $We = 20$) on a heated surface is compared with experiment [7]. The simulation predicts accurately all important details on drop hydrodynamics during the spreading and recoiling such as capillary wave ($t = 1.6$ ms), maximum spreading ($t = 3$ ms) and contact time.

The qualitative comparison between present numerical simulation and temperature contour from high-speed infrared (IR) thermography [7] in Fig 3-b shows good agreement. In the IR images, the visual representation near the interface is blurry and exhibits artificially high and consistent temperatures near the edges of the droplet due the specifics of the experimental setup. To reduce the random error, the central part of the droplet surface is obtained to approximate the droplet mean temperature, so it contains approximately 20% of the inner droplet surface far from edges (for details see [7]),

while in our numerical simulation, drop temperature $T_d = \int T(1+c)/2dV / \int (1+c)/2dV$ is calculated based on the entire droplet volume. In Fig 4, the dimensionless temperature of droplet is plotted from first impingement and rebounding to second impact. At time before the impact or during the spreading phase, when the drop temperature distribution is almost uniform in the droplet, the deviation from experimental data is less significant. In contrast, the maximum mean temperature $T_{d,max}$ strongly deviates from the experiment; this is because the temperature distribution in the drop is highly non-uniform and, in the experiment, hot regions in the droplet bottom are excluded from the estimation of T_d . Furthermore, the gray zone in Fig 4 indicates instances where some parts of droplet are located outside the experiment observation, so a large portion of droplet area is missing.



a) Image sequence of bouncing droplet. Top: experiment [7], bottom: simulation.



b) Temperature contour. Top: experiment recorded by high-speed infrared camera [7], bottom: simulation

Fig.3. Drop ($d_0 = 2.3$ mm, $We=20$, $T_{d,0}=20$ °C) impact on hydrophobic surface ($\theta_e = 140$, $T_s = 60$ °C).

3.2 Heat transfer characteristics

In Fig 5, two thermal boundary conditions at the bottom wall are compared with each other. The surface temperature is slightly cooler when pore cavity exists, however after 12 ms, the surface temperature (T_s) at the bottom remains constant. Therefore, applying the Dirichlet boundary condition instead of implicit boundary condition contributes no major difference in droplet mean temperature. The implicit model is derived based on a Cassie-Baxter condition, it does not account for the possible increase in the effective contact area in Wenzel condition. In order to account for this kind of conditions the explicit (resolved) modeling of the surface structure is inevitable.

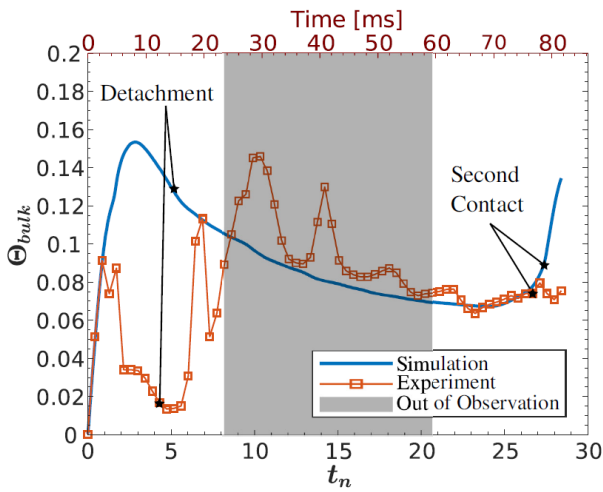


Fig.4: Dimensionless drop temperature $\theta_{bulk} = \frac{T_d - T_{d,0}}{T_s - T_{d,0}}$

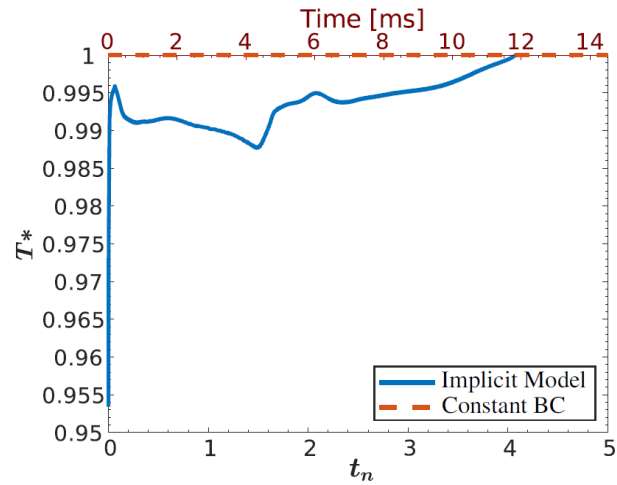


Fig.5: Dimensionless surface temperature $T^* = \frac{T_s - T_{d,0}}{T_{s,0} - T_{d,0}}$. The comparison of surface temperature for implicit and fixed temperature ($T_s = T_{s,0}$)

4. Conclusion

The considered simulations of a drop impact reproduce the experimental observations (droplet hydrodynamics) and can be considered as a complementary tool for experimental studies to overcome experiment limitations. In this study we consider the effect of air entrapment in pore cavity by an implicit model, the result showed it has negligible effect on heat transfer to the droplet. However, to better understand heat transfer rate when a droplet impacts on a superhydrophobic surface, the microtexture topography must be resolved and modelled explicitly.

Acknowledgements

We would like to thank Chunfang Guo for providing additional experimental data. We gratefully acknowledge the financial support by the German Research Foundation (DFG) through the Research Unit 2383 ProMiSe under Grant No. 274353615. In addition, the authors acknowledge support by the state of Baden–Württemberg through bwHPC.

References

- [1] G. Liang and I. Mudawar, "Review of drop impact on heated walls", *International Journal of Heat and Mass Transfer*, vol. 106, pp. 103-126, 2017. Available: 10.1016/j.ijheatmasstransfer.2016.10.031.
- [2] M. Börnhorst and O. Deutschmann, "Single droplet impingement of urea water solution on a heated substrate", *International Journal of Heat and Fluid Flow*, vol. 69, pp. 55-61, 2018. Available: 10.1016/j.ijheatfluidflow.2017.10.007.
- [3] S. Moghtadernejad, C. Lee and M. Jadidi, "An Introduction of Droplet Impact Dynamics to Engineering Students", *Fluids*, vol. 5, no. 3, p. 107, 2020. Available: 10.3390/fluids5030107.
- [4] I. Roisman, "Fast forced liquid film spreading on a substrate: flow, heat transfer and phase transition", *Journal of Fluid Mechanics*, vol. 656, pp. 189-204, 2010. Available: 10.1017/s0022112010001126.
- [5] N. Samkhaniani, A. Stroh, M. Holzinger, H. Marschall, B. Frohnäpfel and M. Wörner, "Bouncing drop impingement on heated hydrophobic surfaces", *International Journal of Heat and Mass Transfer*, vol. 180, p. 121777, 2021. Available: 10.1016/j.ijheatmasstransfer.2021.121777.
- [6] M. Wörner, N. Samkhaniani, X. Cai, Y. Wu, A. Majumdar, H. Marschall, B. Frohnäpfel and O. Deutschmann, "Spreading and rebound dynamics of sub-millimetre urea-water-solution droplets impinging on substrates of varying wettability", *Applied Mathematical Modelling*, vol. 95, pp. 53-73, 2021. Available: 10.1016/j.apm.2021.01.038.
- [7] C. Guo, D. Maynes, J. Crockett and D. Zhao, "Heat transfer to bouncing droplets on superhydrophobic surfaces", *International Journal of Heat and Mass Transfer*, vol. 137, pp. 857-867, 2019. Available: 10.1016/j.ijheatmasstransfer.2019.03.103.